Frontiers in Heat and Mass Transfer

Tech Science Press

https://doi.org/10.32604/fhmt.2026.081417

ARTICLE

Comparative Thermo-Economic Analysis of Standalone and Hybrid Geothermal-Solar Organic Rankine Cycle Systems

Lihan Sun[1], Junze Gong[2], Jinteng Lv[3,*] and Mingfei Mu[3,*]

[1]Inspur Metarnet Communication Information System Co. Ltd., INSPUR GROUP Co. Ltd., Jinan, China
[2]School of Geological Engineering, Qinghai University, Xining, China
[3]Shandong Key Laboratory of Integrated Multi-Energy Systems for High Efficiency and Intelligent Operation/College of Energy Storage Technology, Shandong University of Science and Technology, Qingdao, China

*Corresponding Authors: Jinteng Lv. Email: lvjinteng@outlook.com; Mingfei Mu. Email: mmf@buaa.edu.cn

Received: 02 March 2026; Accepted: 23 April 2026; Published: 29 June 2026

ABSTRACT: Geothermal-solar hybrid power generation has been widely recognized as a promising application within the realm of renewable energy, as such hybridization mitigates solar intermittency while enhancing the utilization of medium-temperature geothermal resources, thus enabling effective energy complementarity. To quantitatively investigate its performance enhancement over single-source systems, this study constructs and analyzes three Organic Rankine Cycle (ORC) based plants with a capacity of approximately 500 kW: a standalone solar ORC, a standalone geothermal ORC, and a hybrid geothermal-solar ORC system. A comprehensive analysis encompassing both design-point and annual off-design operations is conducted, followed by an economic assessment using key metrics. The Lhasa-Yangbajing region in Tibet, China, is selected as the case study due to its abundant geothermal resources and high solar irradiation, providing a representative testing scenario for hybrid energy utilization. At the design point, thermal efficiencies are 12.61% (solar), 6.66% (geothermal), and 9.14% (hybrid). Annual simulation results reflect the impact of solar intermittency, with power generation of 707.26, 4383.3, and 3488.9 MWh, respectively, demonstrating the hybrid system's ability to balance output and stability. Economically, the specific investment costs are 6997.22, 3268, and 4978.4 USD/kWe, and the levelized costs of electricity (LCOE) are 14.09, 1.06, and 2.13 USD/kWh for the solar, geothermal, and hybrid systems. The hybrid configuration offers a favorable trade-off, significantly improving upon the geothermal-only efficiency while drastically reducing costs compared to the single solar system, confirming its substantial integrated application potential.

KEYWORDS: Organic rankine cycle; solar; geothermal; hybrid system

1 Introduction

Electricity serves as a critical foundation for modern industry and societal functioning. In 2022, global electricity generation grew by approximately 2.3%, reaching a total of 29,074 TWh [1]. However, alongside escalating societal and industrial development, the gap between energy demand and supply continues to widen globally [2,3]. This pressing challenge underscores an urgent need to transition the power sector towards green and low-carbon alternatives [4,5]. Enhancing the efficiency of electricity production and developing novel power generation technologies from renewable sources have therefore become imperative [6,7].

Addressing the growing demand for new energy exploitation, the Organic Rankine Cycle (ORC) has garnered significant attention as a flexible and clean power generation technology [8–10]. Its ability to

utilize low-boiling-point organic working fluids [11,12] allows it to be effectively adapted to heat sources with diverse thermodynamic characteristics for efficient power conversion [13,14]. This positions ORC as a particularly advantageous solution for harnessing renewable resources such as solar [15,16] and geothermal energy [17,18]. For the solar ORC, Shi et al. [19] proposed a solar thermal power system based on a parabolic trough collector-ORC platform using R245fa, and the experimental results showed that bypass control stabilizes output at 110~130 W, while system performance is significantly influenced by load conditions and weather variations. In the study of Ren et al. [20], a high-temperature direct steam generation solar power system utilizing a cascade organic Rankine cycle was conducted, which enabled steam generation at 310°C~370°C and achieved a maximum thermal efficiency of 32.85%, potentially offering improved cost-effectiveness compared to conventional direct steaming generation (DSG) plants. For the geothermal ORC, Chitgar et al. [21] conducted a multi-objective optimization of three ORC configurations (basic, parallel, and series) in a geothermal desalination system, and the results showed that the parallel configuration significantly enhances system performance compared to the basic design, with power generation and freshwater production increasing by approximately 150% and 60%, respectively. Liu et al. [22] conducted a comparative evaluation of SORC and RSORC systems driven by geothermal, and the results indicated that R134a achieves the highest net power output and lowest investment cost under most operating conditions, while the RSORC configuration with a recuperator significantly enhances the power output of dry working fluids and reduces parasitic power consumption.

Building upon the extensive research into solar and geothermal ORC applications, a clear synergistic complementarity between these two resources has been identified [23,24]. The efficiency of geothermal plants is often constrained by the moderate temperature of geothermal fluids (typically 100°C~230°C). Conversely, concentrated solar thermal systems can achieve significantly higher temperatures (200°C~500°C) [25,26], offering a potential means to elevate the cycle inlet temperature and thus the performance of a geothermal plant. Meanwhile, the intermittency of solar energy due to diurnal and weather cycles can be mitigated by the continuous, baseload output of geothermal resources. Furthermore, the global distribution of these resources provides a practical foundation for hybrid systems: regions with high solar insolation, such as Australia, the southwestern United States, western China, and northern Africa, frequently coincide with areas rich in geothermal potential [27]. Given these advantages, research and application of geothermal-solar hybrid power systems have expanded rapidly [28]. This development was notably demonstrated by the successful commissioning of the first commercial application at the Stillwater plant in Nevada, USA, in 2015 [29], and the corresponding research was carried out [30,31]. Li et al. [32] proposed a novel solar-enhanced geothermal power generation system based on compound parabolic concentrators, whose net power output reaches 7 to 20 times that of a standalone geothermal system, fully demonstrating the significant advantages of the hybrid power generation approach. Cardemil et al. [33] evaluated the solar-assisted single/double-flash geothermal systems by thermodynamic modeling and the results showed that using solar heat for superheating yields higher power efficiency (0.23~0.29 kWe/kWth) than for evaporation, enabling over 20% additional power, 3% higher exergy efficiency, and 16%~19% reduced geothermal fluid consumption, supporting sustainable reservoir utilization. Shoaei et al. [34] conducted the 4E optimization on a hybrid system by using Non-Dominated Sorting Genetic Algorithm second version (NSGA-II), and the optimal energy efficiency and exergy efficiency were reported with 50.59% and 25.44%, respectively. In the thermo-economic analysis on hybrid system of Boukelia et al. [35], the levelized cost of electricity (LCOE) was evaluated with a value of 10.42 ¢/kWh by using ammonia.

Due to the promising performance of geothermal-solar hybrid power generation, numerous studies have investigated its thermodynamic and economic aspects. Typically, these studies establish a hybrid system based on a geothermal ORC core and report its efficiency gains over the standalone geothermal

plant. However, a comprehensive comparative analysis among hybrid, single geothermal, and single solar ORC systems is often lacking, leaving the extent of performance improvement offered by hybridization insufficiently quantified.

Herein, this study constructs and models three representative ORC-based power plants with a capacity of approximately 500 kW: one geothermal-driven, one solar-driven, and one hybrid-driven, to quantitatively evaluate the thermodynamic and economic advantages of geothermal-solar hybridization in ORC-based power generation, based on the central hypothesis that integrating high-temperature solar thermal energy with a medium-temperature geothermal source can simultaneously enhance system efficiency, mitigate power output fluctuations, and achieve more favorable economic performance than standalone systems. Their performances are systematically compared using a representative working fluid through design-point thermodynamic analysis, annual off-design performance simulations under realistic resource conditions, and a comprehensive thermo-economic assessment based on specific investment cost and the LCOE. The Lhasa-Yangbajing region in Tibet, China, characterized by abundant geothermal resources and high solar irradiation, is selected as a representative case study for evaluating geothermal-solar hybrid energy utilization.

2 Methodology

2.1 Power System

ORC is always considered an effective routine to support the power generation process for solar or geothermal. The ORC system mainly consists of four parts, the pump, the evaporator, the expander, and the condenser, as shown in Fig. 1. The organic working fluids flow through the pump, and then enter into the evaporator to complete the heat absorption from the heat source (solar or geothermal). After that, the working fluids with high pressure and high temperature would drive the expander for power generation. Finally, the working fluids would be cooled in the condenser.

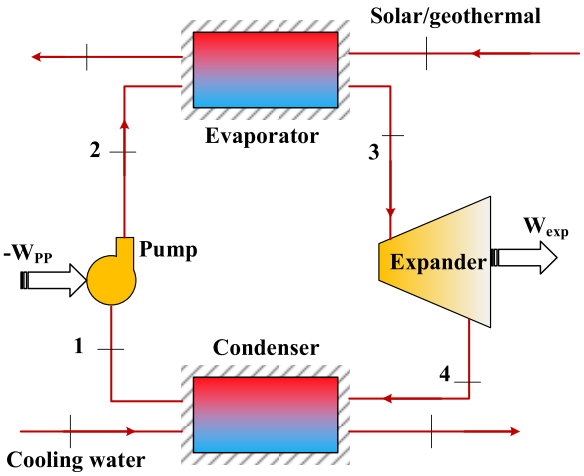

Figure 1: Schematic diagram of the ORC system.

For the heat source concern in this work, the geothermal and solar energy are simultaneously introduced. To compare the system performance, the geothermal, the solar and the geothermal-solar hybrid supported ORC modeling are established. The geothermal ORC system and solar ORC system are operated with the single heat source. In the geothermal-solar hybrid ORC system, the organic working fluid will be sequentially heated by geothermal energy and solar energy in two evaporators connected in series.

For the organic working fluids concern, the safety, environmental friendliness, flexibility and thermodynamic properties are comprehensively considered. The R1233zd(E) with the critical temperature of 165.6°C and the critical pressure of 35.7 bar is selected in the system [36,37], and the corresponding properties are summarized in Table 1.

Table 1: Properties of the employed working fluids.

Name	Type	Critical Point Temperature (°C)	Critical Point Pressure (bar)	GWP100	ODP	ASHREA Safety Classification
R1233zd(E)	Isentropic	165.6	35.7	1	0	A1

Note: ASHRAE: American Society of Heating, Refrigerating and Air-Conditioning Engineers; Global Warming Potential (GWP100); Ozone Depletion Potential (ODP).

2.2 Mathematic Modeling

In order to evaluate the system performance, the system mathematical model is developed, and the thermodynamic and economic characteristics are simultaneously considered, which would be furtherly analyzed based on the software of MATLAB R2019b.

For the solar power system, the parabolic trough solar collector is employed, the incident sunlight is reflected by the parabolic mirror and concentered at a focus line where mounted an absorb tube. The incident solar energy $Q_{sol,incident}$, the absorbed solar energy $Q_{sol,abs}$ by Eqs. (1) and (2). The solar collection efficiency $\eta_{sol,col}$ could be calculated by Eq. (3):

$$Q_{sol,incident} = DNI \cdot A \tag{1}$$

$$Q_{sol,abs} = DNI \cdot A \cdot \eta_{opt} - Q_{loss} \tag{2}$$

$$\eta_{sol,col} = \frac{Q_{sol,abs}}{Q_{sol,incident}} \tag{3}$$

where A and DNI represent the aperture area of solar collector and the direct nominal solar irradiation, respectively; η_{opt} and Q_{loss} denote the optical efficiency and heat loss of the solar collector, respectively.

Correspondingly, the utilized solar energy Q_{sol} can be computed by Eq. (4). For the geothermal power system, and the stable utilized geothermal energy Q_{geo} can be evaluated by Eq. (5):

$$Q_{sol} = m_{wf}\left(h_{eva,out,sol} - h_{eva,in,sol}\right) \tag{4}$$

$$Q_{geo} = m_{wf}\left(h_{eva,out,geo} - h_{eva,in,geo}\right) \tag{5}$$

where the m_{wf} is the mass flowrate of the organic working fluids, and the $h_{eva,out}$ and the $h_{eva,in}$ are the inlet and outlet specific enthalpy of heat exchanger.

For the power modelling, the pump consumption W_{pump} and output of expander $W_{expander}$ could be calculated by Eqs. (6) and (7):

$$W_{pump} = m_{wf}\left(h_{2s} - h_2\right)/\eta_{me,pump}\eta_{ise,pump} = m_{wf}\left(h_{2s} - h_2\right)\eta_{me,pump} \tag{6}$$

$$W_{expander} = m_{wf}\left(h_3 - h_{4s}\right)\eta_{me,exp}\eta_{ise,exp} = m_{wf}\left(h_3 - h_{4s}\right)\eta_{me,exp} \tag{7}$$

where $\eta_{me,pump}$ and $\eta_{me,exp}$ are the mechanical efficiency of the pump and the expander, respectively. h_{2s} and h_{4s} are the state enthalpy with the ideal conversion of the pump and the expander, respectively.

For the system total net power output, consumption of pump and output of expander are included, as computed by Eq. (8). Apart from the pump, the parasitic power consumption W_{para} (with the ratio of 5%) is also need to be considered.

$$W_{\text{net}} = W_{\text{exp ander}} - W_{\text{pump}} - W_{\text{para}} \tag{8}$$

Considering the system overall performances, the first law of thermodynamics is employed, the system energy efficiency $\eta_{\text{th,sys}}$ as the basic evaluation criteria can be expressed as follows:

$$\eta_{\text{th,sys}} = \frac{W_{\text{net}}}{Q_{\text{sol,abs}} + Q_{\text{geo}}} \tag{9}$$

In order to complete the techno-economic analysis on the solar, geothermal and hybrid system, the specific investment cost (SIC) and the LCOE [38] are introduced by Eqs. (10) and (11):

$$\text{SIC} = \frac{C_{\text{invest,device}}}{W_{\text{net}}} \tag{10}$$

$$\text{LCOE} = \frac{C_{\text{invest}}\left(f_{\text{annuity}} + f_{\text{ins,ann}}\right) + \sum_{n}^{N} \frac{C_{\text{O\&M}}}{(1+r)^n}}{W_{\text{net}} \cdot n} \tag{11}$$

where the $C_{\text{invest,device}}$ is the total cost of the employed devices, and the C_{invest}, and $C_{\text{O\&M}}$ represent the capital investment and the annual operation & maintenance cost (with 4% of C_{invest}), the $f_{\text{ins,ann}}$ is the insurance rate with 1%; n and N are the system lifetime with 30 years and the present year, respectively; r is the discount rate with 6%; f_{annuity} represents the investment recovery rate, calculated by Eq. (12) with the interest rate i with 4.2%.

$$f_{\text{annuity}} = \frac{i(1+i)^n}{(1+i)^n - 1} \tag{12}$$

The initial invest of the power system include the cost of ORC devices and the cost of solar field C_{solar} and geothermal field C_{geo}, and the cost of ORC devices insist of the cost of expander C_{exp}, pump C_{pp} and heat exchangers C_{he}, which could be evaluated by Eqs. (13)–(16).

$$C_{\text{invest}} = C_{\text{invest,device}} + C_{\text{solar}} + C_{\text{geo}} = C_{\text{pp}} + C_{\text{exp}} + C_{\text{he}} + C_{\text{solar}} + C_{\text{geo}} \tag{13}$$

$$C_{\text{pp}} = \left(9840 \times \left(0.25 W_{\text{pp}}\right)^{0.55}\right) \times 1.5 \times 1.5 \tag{14}$$

$$C_{\text{exp}} = \left(820 \times W_{\text{exp}}^{0.8} - 19000\right) \times 1.5 \times 1.5 \times 1.6 \tag{15}$$

$$C_{\text{he}} = 235 \times Q^{0.75} \tag{16}$$

2.3 Resources Distribution

Benefited by the geological characteristics, the geothermal resources are abundant in Tibet, China, as shown in Fig. 2a [39,40]. The famous Yangbajing geothermal well is located in Lhasa, Tibet, and the temperature of the outlet geothermal fluids would reach over 150°C. By referring the Yangbajing geothermal power system in Western China [41], the local solar resources are considered for system evaluation with the annual direct irradiation of 6400 MJ/m^2, and the hourly-step DNI profile is shown in Fig. 2b, which are referred by the software of System Advisor Model (SAM). The abundant renewable resources of geothermal and solar energies provide the energy fundament for their hybrid utilization.

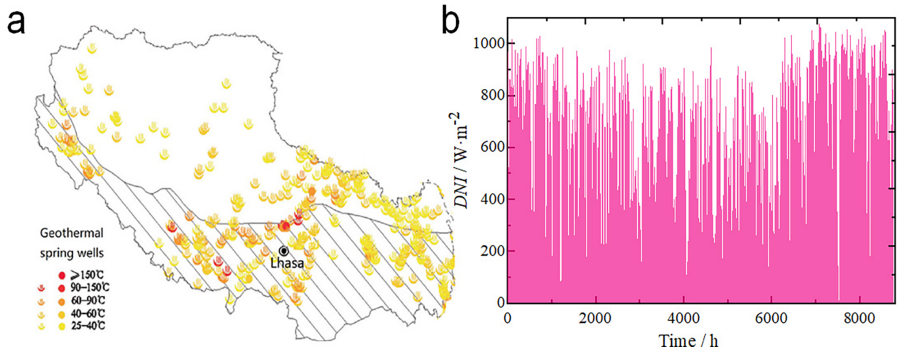

Figure 2: (**a**) Geothermal distribution, (**b**) Solar energy in Lhasa.

3 Results and Discussion

3.1 Designate System Operation Analysis

Based on the local resources in Lhasa, the geothermal-ORC, solar-ORC, and hybrid-ORC configuration are established, and the designate system capacity are aimed at 500 kW. The corresponding parameters are summarized in Table 2. For the geothermal ORC, the brine temperature with 145°C referencing the Yangbajing geothermal field, requiring a 7510 kW heat input at a 70°C evaporation temperature. The solar ORC employs parabolic trough collectors with thermal conductive oil (240°C), needing a 3970 kW input at a 120°C evaporation temperature. The hybrid system synergistically combines both sources at half their standalone inputs (3755 kW geothermal and 1985 kW solar), operating at an optimized evaporation temperature of 90°C to efficiently utilize the complementary thermal profiles.

Table 2: Operation parameter of the geothermal, solar and hybrid system.

	Geothermal-ORC	Solar-ORC	Hybrid-ORC
Temperature of heat source/°C	145	240	145/240
Heat input/kW	7510	3970	3755/1985
Evaporation temperature/°C	70	120	90
Inlet temperature of expander/°C	120	180	207
Isentropic efficiency of pump	80%	80%	80%
Isentropic efficiency of expander	80%	80%	80%

According to designate operating parameters, the T-s diagrams are carried out in Fig. 3, which depict the operational cycles for the three systems under design conditions. Compared to the geothermal and hybrid cycles, the solar ORC operates at a higher temperature, which creates a greater temperature differential during evaporation. This leads to significant irreversible heat transfer losses. Consequently, despite utilizing a higher-grade heat source, the standalone solar system exhibits lower overall energy utilization efficiency than both the geothermal and hybrid configurations.

Under the design conditions, the operational performance of the three systems is presented in Fig. 4. Both the geothermal and solar ORC systems achieve the target power output of 500 kW, with thermal efficiencies of 6.66% and 12.61%, respectively. Owing to the higher temperature of the solar heat source, the solar ORC operates at a higher permissible evaporation temperature, resulting in a significantly superior thermal efficiency compared to the geothermal system. The hybrid system delivers a power output of

524.60 kW, slightly exceeding the design target. Its thermal efficiency is 9.14%, which lies between that of the two standalone systems, reflecting the integrated performance achieved through source complementarity and parameter optimization.

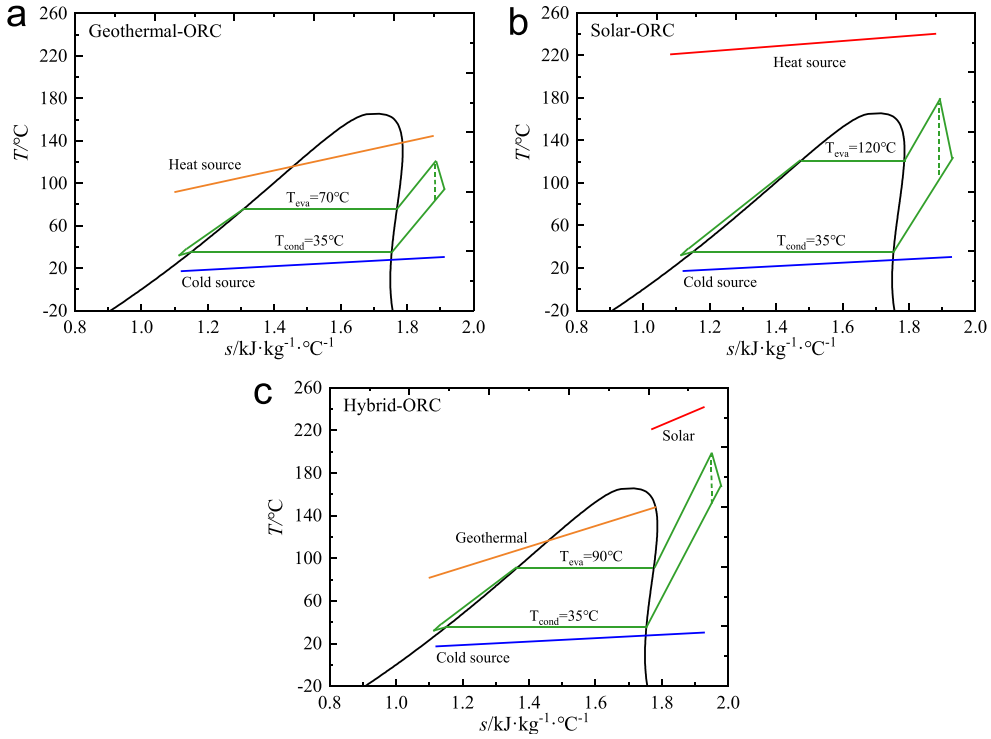

Figure 3: T-s diagram. (**a**) Geothermal power system, (**b**) Solar power system, (**c**) Geothermal-solar hybrid system.

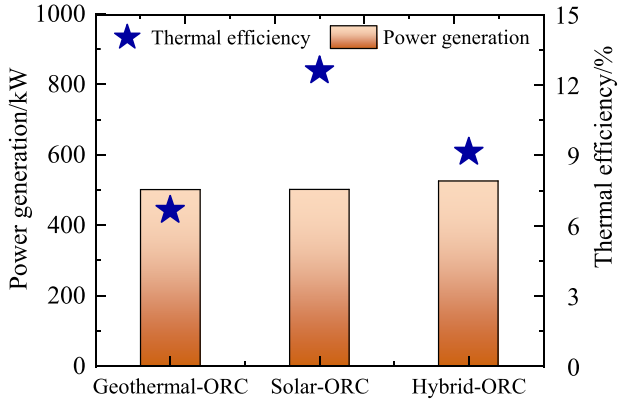

Figure 4: System performance comparison on designate condition.

In ORC systems, the evaporation temperature is a key parameter influencing system performance. As shown in Fig. 5, both the net power output and thermal efficiency of all three systems increase with rising evaporation temperature. This trend occurs because a higher evaporation temperature reduces the temperature difference during heat exchange with the heat source, thereby decreasing irreversible losses and improving the utilization of thermal energy. Since all three systems employ R1233zd(E) as the working fluid,

they exhibit similar thermal efficiencies at the same evaporation temperature. However, due to its larger designed heat input, the geothermal ORC achieves a higher power output under identical conditions.

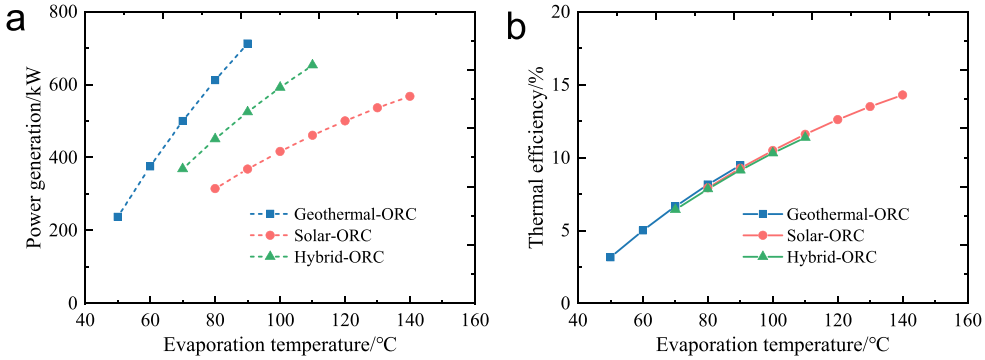

Figure 5: Effect of the evaporation temperature on system performance. (**a**) Power generation, (**b**) Thermal efficiency.

3.2 The Annual System Operation Analysis

The performance of solar-integrated power generation systems under fluctuating solar radiation is a key focus of investigation. In this section, the solar field is modeled based on the solar conditions in the Lhasa region to analyze the annual operational performance of both the solar ORC and the hybrid ORC systems. For the system operation strategy in this work, the superheating temperature in evaporation process of the ORC system would be reduced with the decreasing solar collection. When the superheat drops below 0°C, the ORC system ceases operation. Besides, in the hybrid power generation system, solar energy only supplies heat for the superheating part of the working fluid. Therefore, even if the solar heat collection is 0 kW, the ORC system can still maintain continuous operation with the support of geothermal energy. A comparative assessment of the yearly operating results for all three systems is subsequently conducted.

Fig. 6 presents the annual instantaneous solar thermal collection efficiency. Overall, the collection efficiency is higher during summer and autumn, reaching nearly 70%. In contrast, it significantly deteriorates in winter due to changes in solar altitude angle. The annual average collection efficiency for the system is 49.77%.

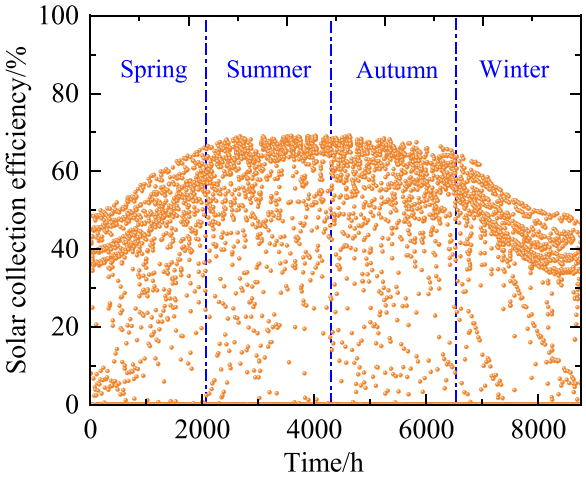

Figure 6: The annual instantaneous solar thermal collection efficiency.

Based on the solar thermal requirements of the solar and hybrid ORC systems under design conditions, a solar collector field was designed using a DNI of 850 W/m^2. The required collector areas were determined to be 10,496 and 5248 m^2 for the standalone solar and hybrid systems, respectively. The annual solar heat collection, contrasted with the stable geothermal input of approximately 7510 kW, is presented in Fig. 7, indicating that while the geothermal input remains constant, the total thermal energy input for the solar-integrated systems exhibits significant dynamic fluctuation due to solar intermittency. Crucially, since the power block capacity is fixed, there is a maximum limit on the usable solar heat even during periods of high insolation. Consequently, the instantaneous total thermal input varies between 0~3970 kW of the design capacity for the solar ORC and between 3755~5740 kW for the hybrid system.

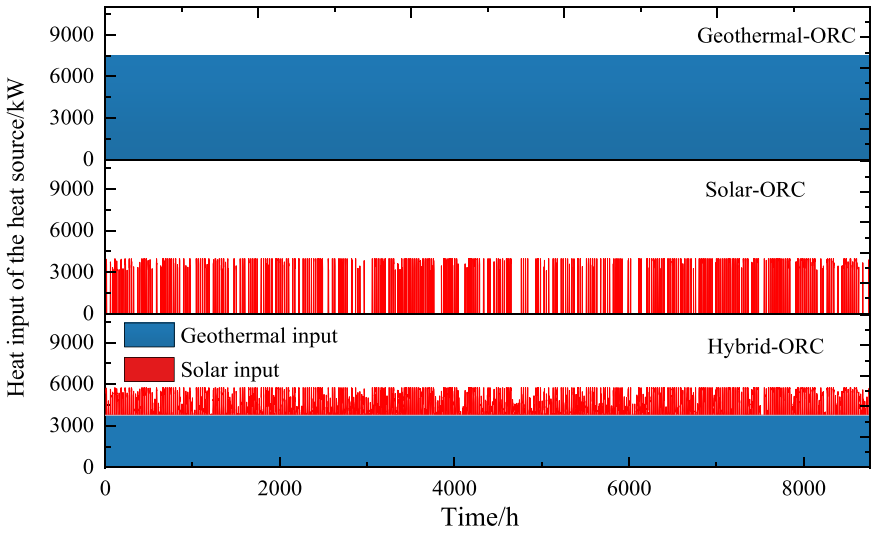

Figure 7: Comparison of heat input of the heat source across the established configurations.

As shown in Fig. 8, the power generation response of the systems aligns closely with the fluctuating energy inputs from Fig. 7. The hourly power output is stable at 500 kW for the geothermal ORC, fluctuates between 0 and 500 kW for the solar ORC, and ranges from 356.74 to 524.60 kW for the hybrid system. For the hybrid configuration, its nighttime operation is guaranteed by a stable geothermal baseload, providing a minimum output of 356.74 kW, while higher daytime power generation is achieved by integrating the higher-grade solar heat.

Based on the annual simulation results, the thermodynamic performance of the three systems is summarized in Table 3. The annual power generation for the geothermal, solar, and hybrid ORC systems is 4380.3, 707.26, and 3488.9 MWh, with corresponding annual average thermal efficiencies of 6.66%, 7.62%, and 9.41%, respectively.

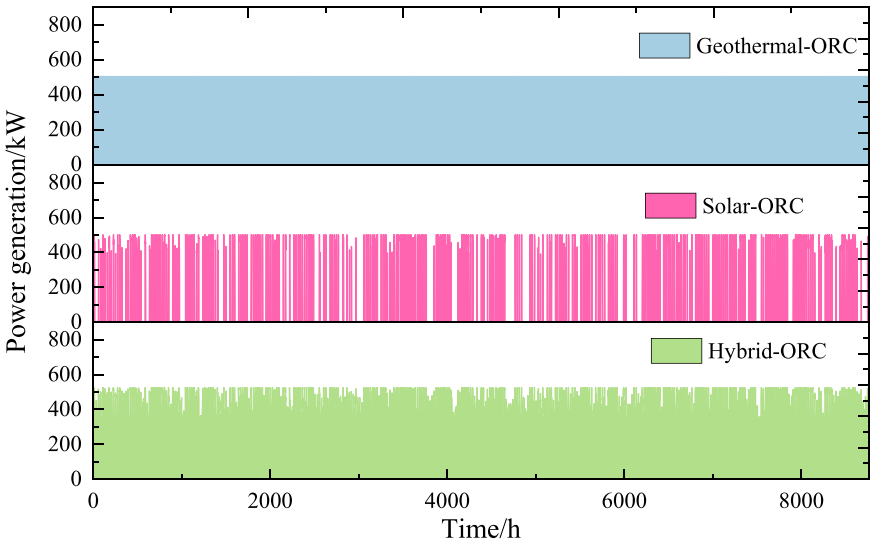

Figure 8: Comparison of power generation across the established configurations.

Table 3: The annual system operation performance.

	Geothermal-ORC	Solar-ORC	Hybrid-ORC
Power generation/MWh	4380.3	707.26	3488.9
Thermal efficiency/%	6.66	7.62	9.41

3.3 The Economic Analysis

To further evaluate the performance of the hybrid ORC, a thermo-economic analysis is conducted using the specific investment cost and LCOE models, with initial investment costs detailed in Table 4.

Table 4: Initial ingestion of the system.

	Cost	Unit
Solar field [33]	250	USD/m^2
Geothermal field [40]	100	USD/kWhth
Expander [41,42]	$(820 \times W^{0.8} - 19{,}000) \times 1.5 \times 1.5 \times 1.6$	USD/kWhe
Pump [41,42]	$(9840 \times (0.25W)^{0.55}) \times 1.5 \times 1.5$	USD/kWhe
Heat exchanger [41]	$235 \times Q^{0.75}$	USD/kWhth

The initial investment costs for key system components are compared in Fig. 9. The results indicate total capital costs of 1527, 3269.73, and 2440.08 kUSD for the geothermal ORC, solar ORC, and hybrid systems, respectively. Notably, the solar collector field constitutes a major cost factor, accounting for over half of the total expense in the solar ORC system. By integrating the lower-cost geothermal component, the hybrid system achieves a significant reduction in overall capital investment.

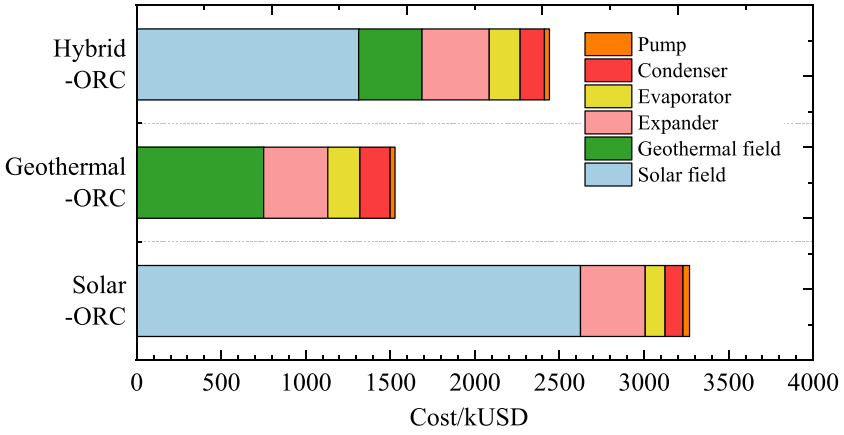

Figure 9: Cost of the crucial device.

The thermo-economic analysis results for the three systems are presented in Fig. 10. In terms of specific investment cost, the values are 3268, 6997.22, and 4978.4 USD/kWe for the geothermal, solar, and hybrid ORC systems, respectively. The solar ORC demonstrates significantly weaker economic performance compared to the geothermal system, a finding further corroborated by the LCOE results of 1.06, 14.09, and 2.13 USD/kWh for the respective systems. Overall, the hybrid system exhibits a clear advantage when considering both thermo-dynamic efficiency and economic metrics. While the geothermal system is constrained by its low-temperature heat source, limiting efficiency gains, the solar ORC suffers from intermittency and the high capital cost of its collector field. The latter's economics could potentially be improved through the integration of thermal storage in future work.

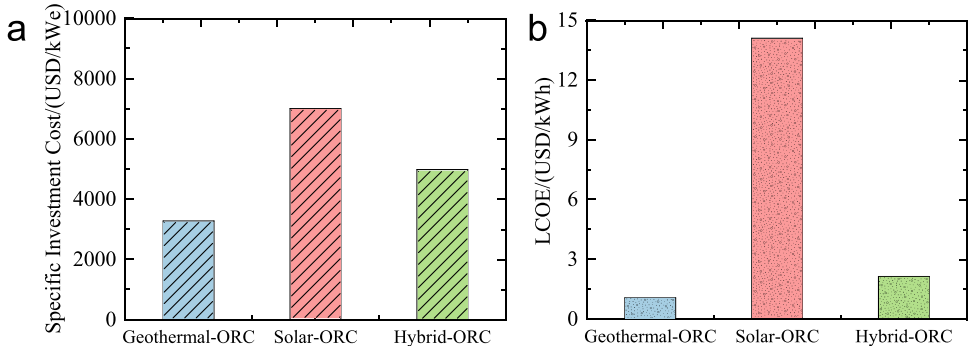

Figure 10: The comprehensive tech-economic result. (**a**) Specific investment cost, (**b**) LCOE.

4 Conclusions

In this work, three ORC systems (solar, geothermal, and hybrid) are conducted. The system operation under designate and off-designate conditions are compared, and a corresponding thermo-economic assessment is carried out. The main conclusions are summarized as follows:

(1) By considering the geothermal and solar energy with 145°C and 240°C, the thermal efficiency of the solar-ORC, geothermal-ORC, and hybrid ORC are 12.61%, 6.66%, 9.14%, respectively, with the corresponding evaporation temperature at 120°C, 70°C, 90°C.

(2) Based on the varying solar radiation, the annual power generation of the solar, geothermal, and hybrid ORC systems is 707.26, 4383.3, and 3488.9 MWh, respectively. This result highlights the complementary role of geothermal in mitigating solar intermittency.

(3) The thermo-economic analysis yields specific investment costs of 6997.22, 3268, and 4978.4 USD/kWe and LCOE of 14.09, 1.06, and 2.13 USD/kWh for the solar, geothermal, and hybrid systems, respectively. The hybrid configuration presents a favorable trade-off, demonstrating significant application potential.

The proposed hybrid ORC system can be modularly scaled by adjusting geothermal and solar heat inputs according to local resource availability, enabling flexible deployment in regions with medium-temperature geothermal resources and high solar irradiation. Existing geothermal plants can be retrofitted with solar thermal fields to enhance performance without major modifications to the power block, reducing technical and financial barriers. From a policy perspective, the results support integrating geothermal-solar hybrid systems into renewable energy incentive schemes and long-term power planning, while future work should focus on thermal energy storage integration, advanced off-design control, and life-cycle environmental assessment to further enhance system performance and sustainability.

Acknowledgement: Not applicable.

Funding Statement: This work was supported by the National Natural Science Foundation of China (No. 52106091).

Author Contributions: Conceptualization, Mingfei Mu; methodology, Lihan Sun; software, Junze Gong; validation, Lihan Sun; investigation, Junze Gong; data curation, Mingfei Mu; writing—original draft preparation, Mingfei Mu and Lihan Sun; writing—review and editing, Jinteng Lv; project administration, Jinteng Lv; funding acquisition, Jinteng Lv. All authors reviewed and approved the final version of the manuscript.

Availability of Data and Materials: The original contributions presented in the study are included in the article, further inquiries can be directed to the corresponding authors.

Ethics Approval: Not applicable.

Conflicts of Interest: The authors declare no conflicts of interest.

References

1. International Energy Agency. Coal 2023 [Internet]. [cited 2026 Apr 1]. Available from: https://www.iea.org/reports/coal-2023.
2. International Energy Agency. Electricity market report 2023 [Internet]. [cited 2026 Apr 1]. Available from: https://www.iea.org/reports/electricity-market-report-2023.
3. Wang Y, Hu H, Wang X, Liu H, Dong L, Luo G, et al. A critical review on lead migration, transformation and emission control in Chinese coal-fired power plants. J Environ Sci. 2023;124:397–413. doi:10.1016/j.jes.2021.09.039.
4. Bilgili M, Ozbek A, Sahin B, Kahraman A. An overview of renewable electric power capacity and progress in new technologies in the world. Renew Sustain Energy Rev. 2015;49:323–34. doi:10.1016/j.rser.2015.04.148.
5. Manzano-Agugliaro F, Alcayde A, Montoya FG, Zapata-Sierra A, Gil C. Scientific production of renewable energies worldwide: an overview. Renew Sustain Energy Rev. 2013;18(9):134–43. doi:10.1016/j.rser.2012.10.020.
6. Li G, Xu J, Liu S, Zhao D, Zheng Y, Guo W. High-energy density micro swirl combustion powered thermoelectric generator for combined heat and power supply. Therm Sci Eng Prog. 2025;68:104369. doi:10.1016/j.tsep.2025.104369.
7. Gao Y, Tahir M, Siano P, Hussain S, Sun W, He Y, et al. A bi-level hybrid game framework for Stochastic Robust optimization in multi-integrated energy microgrids. Sustain Energy Grids Netw. 2025;44(1):102024. doi:10.1016/j.segan.2025.102024.

8. Farhat O, Faraj J, Hachem F, Castelain C, Khaled M. A recent review on waste heat recovery methodologies and applications: comprehensive review, critical analysis and potential recommendations. Clean Eng Technol. 2022;6:100387. doi:10.1016/j.clet.2021.100387.
9. Wieland C, Schifflechner C, Dawo F, Astolfi M. The organic Rankine cycle power systems market: recent developments and future perspectives. Appl Therm Eng. 2023;224(10):119980. doi:10.1016/j.applthermaleng.2023.119980.
10. Loni R, Najafi G, Bellos E, Rajaee F, Said Z, Mazlan M. A review of industrial waste heat recovery system for power generation with Organic Rankine Cycle: recent challenges and future outlook. J Clean Prod. 2021;287:125070. doi:10.1016/j.jclepro.2020.125070.
11. Chen H, Goswami DY, Stefanakos EK. A review of thermodynamic cycles and working fluids for the conversion of low-grade heat. Renew Sustain Energy Rev. 2010;14(9):3059–67. doi:10.1016/j.rser.2010.07.006.
12. Bao J, Zhao L. A review of working fluid and expander selections for organic Rankine cycle. Renew Sustain Energy Rev. 2013;24(8):325–42. doi:10.1016/j.rser.2013.03.040.
13. Zhang YF, Li MJ, Ren X, Duan XY, Wu CJ, Xi H, et al. Effect of heat source supplies on system behaviors of ORCs with different capacities: an experimental comparison between the 3 and 10 kW unit. Energy. 2022;254:124267. doi:10.1016/j.energy.2022.124267.
14. Liu H, Lu B, Xu Y, Ju X, Wang W, Zhang Z, et al. Experimental investigation of a splitting organic Rankine cycle for dual waste heat recovery. Energy Convers Manag. 2024;320:119005. doi:10.1016/j.enconman.2024.119005.
15. Liu Z, Guan H, Jin X, Su W, Shao J, Fan J, et al. Thermodynamic and economic analysis of a trans-critical CO_2 energy storage system integrated with ORC and solar energy. Energy. 2024;313(62):133667. doi:10.1016/j.energy.2024.133667.
16. Shi X, Wang X, Zhang C, Wang F. Numerical analysis on the performance of an ORC system based on solar concentration and spectrum utilization. Renew Energy. 2026;256(1):124435. doi:10.1016/j.renene.2025.124435.
17. Maghfuri AM. Developing geothermal ORC power plant using different CFCs fluids: case study in Saudi Arabia. Therm Sci Eng Prog. 2025;65:103939. doi:10.1016/j.tsep.2025.103939.
18. Tomasini-Montenegro C, Santoyo-Castelazo E, Gujba H, Romero RJ, Santoyo E. Life cycle assessment of geothermal power generation technologies: an updated review. Appl Therm Eng. 2017;114:1119–36. doi:10.1016/j.applthermaleng.2016.10.074.
19. Shi X, Jiang W, Wang X, Zhang C. Experimental and numerical investigations of an ORC power generation system based on solar concentration and heat collection technology. Appl Therm Eng. 2025;281:128642. doi:10.1016/j.applthermaleng.2025.128642.
20. Ren X, Li J, Gao G, Pei G. An innovative concentrated solar power system driven by high-temperature cascade organic Rankine cycle. J Energy Storage. 2022;52:104999. doi:10.1016/j.est.2022.104999.
21. Chitgar N, Hemmati A, Sadrzadeh M. A comparative performance analysis, working fluid selection, and machine learning optimization of ORC systems driven by geothermal energy. Energy Convers Manag. 2023;286:117072. doi:10.1016/j.enconman.2023.117072.
22. Liu Q, Yang F, Liu X, Zhang X, Yang Z. Thermo-economic evaluation and working fluid screening for supercritical ORCs driven by medium-temperature geothermal sources. Renew Energy. 2026;257(2):124795. doi:10.1016/j.renene.2025.124795.
23. Wainaina Kariuki B, Hassan H, Ahmed M, Emam M. A review on geothermal-solar hybrid systems for power production and multigeneration systems. Appl Therm Eng. 2025;259:124796. doi:10.1016/j.applthermaleng.2024.124796.
24. Mahmoudan A, Esmaeilion F, Hoseinzadeh S, Soltani M, Ahmadi P, Rosen M. A geothermal and solar-based multigeneration system integrated with a TEG unit: development, 3E analyses, and multi-objective optimization. Appl Energy. 2022;308(280):118399. doi:10.1016/j.apenergy.2021.118399.
25. He YL, Qiu Y, Wang K, Yuan F, Wang WQ, Li MJ, et al. Perspective of concentrating solar power. Energy. 2020;198:117373. doi:10.1016/j.energy.2020.117373.
26. Khan J, Arsalan MH. Solar power technologies for sustainable electricity generation—a review. Renew Sustain Energy Rev. 2016;55(4):414–25. doi:10.1016/j.rser.2015.10.135.

27. Wang F, Cheng Z, Tan J, Yuan Y, Shuai Y, Liu L. Progress in concentrated solar power technology with parabolic trough collector system: a comprehensive review. Renew Sustain Energy Rev. 2017;79(6):1314–28. doi:10.1016/j.rser.2017.05.174.
28. Hu S, Yang Z, Li J, Duan Y. Thermo-economic optimization of the hybrid geothermal-solar power system: a data-driven method based on lifetime off-design operation. Energy Convers Manag. 2021;229(41):113738. doi:10.1016/j.enconman.2020.113738.
29. Pramanik S, Ravikrishna RV. A review of concentrated solar power hybrid technologies. Appl Therm Eng. 2017;127:602–37. doi:10.1016/j.applthermaleng.2017.08.038.
30. Kariuki BW, Emam M, Hassan H. Parametric assessment of solar and geothermal standalone hybrid system for power, green hydrogen, and freshwater production. Renew Energy. 2026;256:124270. doi:10.1016/j.renene.2025.124270.
31. Bozkurt A, Genç MS, Seyitoğlu SS. 7E analysis of a low-temperature geothermal and solar energy integrated hybrid system for sustainable power and hydrogen generation. Therm Sci Eng Prog. 2025;66(8):104073. doi:10.1016/j.tsep.2025.104073.
32. Li T, Liang X, Zhou K, Wang J. Technical performance of a novel solar-enhanced geothermal power generation system in China. Case Stud Therm Eng. 2025;74(1):107017. doi:10.1016/j.csite.2025.107017.
33. Cardemil JM, Cortés F, Díaz A, Escobar R. Thermodynamic evaluation of solar-geothermal hybrid power plants in northern Chile. Energy Convers Manag. 2016;123:348–61. doi:10.1016/j.enconman.2016.06.032.
34. Shoaei M, Hajinezhad A, Moosavian SF. Design, energy, exergy, economy, and environment (4E) analysis, and multi-objective optimization of a novel integrated energy system based on solar and geothermal resources. Energy. 2023;280(10):128162. doi:10.1016/j.energy.2023.128162.
35. Boukelia TE, Arslan O, Djimli S, Kabar Y. ORC fluids selection for a bottoming binary geothermal power plant integrated with a CSP plant. Energy. 2023;265(10):126186. doi:10.1016/j.energy.2022.126186.
36. Liu J, Zhang Y, Li H, Shuai Y, Li B, Hung TC. Low-grade thermal energy utilization through using organic Rankine cycle system and R1233zd(E) at different heat source temperatures. Appl Therm Eng. 2023;230(5):120706. doi:10.1016/j.applthermaleng.2023.120706.
37. Eyerer S, Dawo F, Kaindl J, Wieland C, Spliethoff H. Experimental investigation of modern ORC working fluids R1224yd(Z) and R1233zd(E) as replacements for R245fa. Appl Energy. 2019;240(C):946–63. doi:10.1016/j.apenergy.2019.02.086.
38. Bonyadi N, Johnson E, Baker D. Technoeconomic and exergy analysis of a solar geothermal hybrid electric power plant using a novel combined cycle. Energy Convers Manag. 2018;156(1):542–54. doi:10.1016/j.enconman.2017.11.052.
39. Wang X, Wang G, Lu C, Gan H, Liu Z. Evolution of deep parent fluids of geothermal fields in the Nimu–Nagchu geothermal belt, Tibet, China. Geothermics. 2018;71(1):118–31. doi:10.1016/j.geothermics.2017.07.010.
40. Li D, Rao Z, Zhuo Q, Chen R, Dong X, Liu G, et al. Resource endowments effects on thermal-economic efficiency of ORC-based hybrid solar-geothermal system. Case Stud Therm Eng. 2023;52:103739. doi:10.1016/j.csite.2023.103739.
41. Gong L, Zhang Y, Bai Z. Geothermal-solar hybrid power with the double-pressure evaporation arrangement and the system off-design evaluation. Energy Convers Manag. 2021;244(14–15):114501. doi:10.1016/j.enconman.2021.114501.
42. Van Erdeweghe S, Van Bael J, Laenen B, D'Haeseleer W. Feasibility study of a low-temperature geothermal power plant for multiple economic scenarios. Energy. 2018;155:1004–12. doi:10.1016/j.energy.2018.05.028.